Front. Mater. Sci. 2017, 11(3): 296–305
DOI 10.1007/s11706-017-0387-7

RESEARCH ARTICLE

# Dynamic recrystallization behavior of AZ31 magnesium alloy processed by alternate forward extrusion

Feng LI (✉), Yang LIU, and Xu-Bo LI

School of Materials Science and Engineering, Harbin University of Science and Technology, Harbin 150040, China



**ABSTRACT: One of the important factors that affect the microstructure and properties of extruded products is recrystallization behavior. Alternate forward extrusion (AFE) is a new type of metal extrusion process with strong potential. In this paper, we carried out the AFE process experiments of as-cast AZ31 magnesium alloy and obtained extrusion bar whose microstructure and deformation mechanism were analyzed by means of optical microscopy, electron backscattered diffraction and transmission electron microscopy. The experimental results indicated that homogeneous fine-grained structure with mean grain size of 3.91 μm was obtained after AFE at 573 K. The dominant reason of grain refinement was considered the dynamic recrystallization (DRX) induced by strain localization and shear plastic deformation. In the 573–673 K range, the yield strength, tensile strength and elongation of the composite mechanical properties are reduced accordingly with the increase of the forming temperature. Shown as in relevant statistics, the proportion of the large-angle grain boundaries decreased significantly. The above results provide an important scientific basis of the scheme formulation and active control on microstructure and property for AZ31 magnesium alloy AFE process.**

**KEYWORDS: magnesium alloy; alternate forward extrusion (AFE); mechanical property; dynamic recrystallization**

## Contents



Received May 6, 2017; accepted June 12, 2017

E-mail: fli@hrbust.edu.cn

## 1 Introduction

Nowadays, the requirements of lightweight products in industrial applications can achieve usually through optimizing products structure and using lightweight materials. But for the majority products with a fixed structure, using lightweight materials is the ideal choice and has a more profound significance in view of applicability. As the lightest metal structural materials in the engineering

application to date [1–3], magnesium alloy has many excellent properties and is widely used for manufacturing in aerospace, transportation, military equipment, and other fields.

But hexagonal close-packed (hcp) structure determines the magnesium alloy poorer plastic deformation ability at room temperature, which is a mainly reason restricted the manufacture of bearing components. The activation of prismatic slip and pyramidal slip when the grains refine to a certain extent can improve strength and toughness of magnesium alloy. Severe plastic deformation (represented by equal-channel angular pressing (ECAP) [4], cyclic extrusion compression (CEC) [5] and high-pressure torsion (HPT) [6]) which provides an effective way for the preparation of high performance fine grain magnesium alloy attracted a lot of people to join in the research area. But now the existing severe plastic deformation (SPD) technology still need to repeatedly machining the billets [7–9], so SPD technology is currently limited to the use of the laboratory stage and needs to solve some bottlenecks for the application of industrialization because of wasting time and energy.

In view of the above problems, ongoing attempts have been made by different investigators in order to achieve the precision integration control of the shape and performance simultaneously in single pass extrusion process [10]. The purpose of this work is to actualize the effective connection between the preparation of high performance fine grain structure and the subsequent "machining and forming" process, which is also one of the hot research directions in this field. Sepahi-Boroujeni et al. [11] added an expansion cavity at the connection of two intersecting channels in ECAP based on ECAP mold structure. The remedy improved the microstructure and enhanced the comprehensive performance of the product due to result in the induction of larger strains and make the fluidity of metals complicated. Hu et al. [12] proposed the extrusion-shear composite extrusion (EC) process of combining with conventional extrusion (CE) and ECAP which included two simple shear extrusion processes compared with the CE. The average grain size of the recrystallized structure obtained by EC process is about 2 μm and the grain refinement ability is better than the CE. However, it is limited to the experimental research stage and cannot be carried out in actual mass production at present. Orlov et al. [13–14] combined CE and the traditional ECAP producing ZK60 magnesium alloy products in a single processing step. And the extrudate exhibited an excellent the comprehensive performance advantage, such as yield and tensile strength reached 310 and 351 MPa respectively, and total elongation was 2.5 times than that of the initial billet. Shahbaz et al. [15] designed stationary die which eliminates the slippage problem in torsion extrusion method and simplifies the processing operation. Vortex extrusion (VE) as a new SPD technique benefits from simultaneous torsion and extrusion of samples. The research can obtain up to 6.4 high uniform strain distributions and the effect of fine grain can be remarkably improved. The asymmetric design for extrusion die orifice can increase shear strain leading to an almost full evolution of equiaxial fine grains. The new grain evolution can be controlled by a series of strain-induced continuous dynamic recrystallization (CDRX) [16]. The method can effectively weaken the basal texture and improve the ductility at room temperature. Yang et al. [17] shown that, compared with CE, asymmetric shear deformation in asymmetric extrusion could remarkably weaken strength of the (0002) basal texture. Furthermore, it enforces the crystallographic reorientation of basal planes to tilt about 12° toward the extrusion direction. Differences of velocity in different parts of the die orifice caused additional asymmetric shear deformation [18]. The method generated DRX and achieved grain refinement. So the room temperature strength and ductility of AZ31 magnesium alloy significantly improved.

As a result, the severe plastic strain is introduced due to the unique design of the die structure, which provides the source power for the grain refinement in the extrusion process [19–20]. In order to find a more effective way for the actual production, the alternate forward extrusion (AFE) method came into being. AFE can simplify the process and increase shear deformation in single pass extrusion process, which provides the possibility of improving grain refining ability. In this paper, through the evaluation and analysis of the extrusion parts at different temperatures, the influence law of forming temperature on the microstructure of AFE is obtained.

## 2 Experimental

### 2.1 Process principle

Compared with the traditional concept of extrusion technology, the biggest difference was that the punch was designed into two symmetrical sub-structures in the AFE process. Punches in the AFE process applied load down-

ward alternately. The schematic of AFE was shown in Fig. 1. A full load pass included two steps that the left punch moved downward for *h* and was fixed then the right punch moved downward to the same position subsequently. We completed the AFE experiment which included a total of 3 passes.

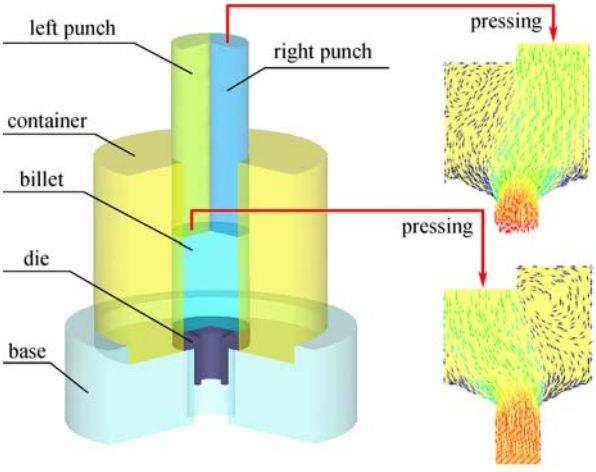


**Fig. 1** The schematic of AFE.

The advantages of the process were as follows. When separate punch moved alternately downward in half pass, the actual loading function area decreased significantly compared with CE. Therefore, the forming load was significantly reduced. In addition severe shear deformation at the interface of different punch end refined the billet internal organization deeply. Theoretical analysis showed that the unique design of double split punches made internal organization of extruded rod more homogenized. At the same time, double ends of the billet are deformed by shear deformation, so that the microstructure is refined compared with CE in which the grains are refined only at the die. The metal flow behavior and order in the mold cavity are changed when the two punches are alternately loaded. Not only the "S-shaped" split-flow surface is produced, but also the "vortex" behavior is produced at the end of side punch when the punch is loaded. This is a unique phenomenon in the process of AFE. The range of eddy current behavior is directly related to the unilateral punch load. The range of "vortex" behavior is directly related to the single pass press length *h*.

## 2.2 Materials and methods

Commercial casting feedstock of AZ31 alloys rod was used for the sample material in the present study, and the chemical compositions are shown in Table 1.

**Table 1** AZ31 magnesium alloy compositions

| Chemical composition | Content /wt.% |
|---|---|
| Al | 3.20 |
| Zn | 0.86 |
| Mn | 0.36 |
| Fe | 0.0018 |
| Si | 0.021 |
| Cu | 0.0022 |
| Ni | 0.00056 |
| Mg | bal. |

Cast rod was lathed to ingots with dimensions of Φ40 mm × 50 mm. Then the ingots were homogenized treatment at 420°C for 12 h followed by cooling to room temperature before extruded. Water-based graphite was used as a lubricant. AFE were performed at different temperatures of 300°C, 350°C and 400°C, respectively. Prior to the AFE processing, the ingot and the die were preheated to predetermined temperature 300°C and kept isothermally for 30 min. By exploiting a thermocouple at the die and close enough to the deformation zone, the temperature was monitored and controlled to vary within ±2°C. According to the relatively low stroke speed the temperature increasing during extrusion was ignored. Single pass press length *h* set to 10 mm and its extrusion ratio was 8.16. AFE was carried out at an extrusion rate of 1 mm/s of the punch at 300°C and the extruded products were quenched in water. Then, the temperature adjusted in turn to 350°C and 400°C and repeated the above steps until completing the technology experiment.

Figure 2 shows the die structure and the extrusion extrudate. Compared with the CE, when split punches alternately apply downward loading during the AFE process will change the stress state of ingot. The extrusion extrudate obtained by using the conventional die for AFE has obvious periodic bending defect in Figs. 2(a) and 2(b) if no other special measures are taken. The length of the adjacent inflection points is related to the single pass press length *h*. Although the defect can be treated by straightening process, it will inevitably have adverse effects on the mechanical properties of the extrudate. Figures 2(c) and 2(d) are shown to avoid the occurrence of the bending defects when the conventional die is added with a length of 20 mm oriented part.

After the extrusion tests, optical microscopy (OM) and electron backscattered diffraction (EBSD) were conducted for microstructure analyses. The extrusion direction (ED), normal direction (ND) and transverse direction (TD) were shown in Fig. 2. Specimens for OM and EBSD were cut

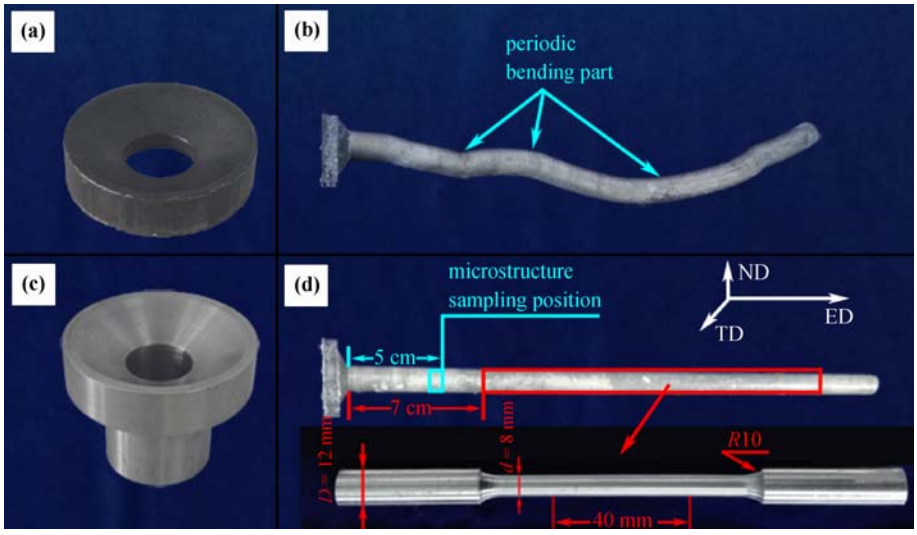


**Fig. 2** Dies structure and extruded products: **(a)** conventional die; **(b)** extrusion extrudate using traditional die; **(c)** oriented die; **(d)** extrusion extrudate using oriented die.

from center of the extruded rods cross section; the observation planes were along vertical extrusion direction plane (ND and TD plane) and parallel to the extrusion direction plane (ED and TD plane) respectively. Specimens for OM were ground with 1200 grit SiC paper, and then mechanically polished using diamond paste. Specimens were etched in a solution of 1 mL acetic acid, 1 mL nitric acid, 1 g oxalic acid and 150 mL water. Specimens for EBSD were ground with 2000 grit SiC paper, followed by mechanically polishing by diamond paste. Specimens were prepared by electro-polishing in an electrolyte solution which consisted of phosphoric acid and ethyl alcohol (volume ratio 3:5) at 0.5 A for 2 min and then at 0.2 A for 3 min for the final stage. The EBSD tests were carried out by a 200°F Quanta field emission environmental scanning electron microscope, and the experimental data were analyzed by OIM Analysis TSL 6 software. The step size of EBSD measurements was 1.3 μm. The tensile property test was done along the ED. Tensile samples were machined to cylindrical with gauge length of Φ8 mm × 40 mm and tensile test carried out at room temperature with a strain rate of $1\times10^{-3}$ $s^{-1}$. Then scanning electronic microscopy (SEM) was used for observing the fracture morphology. The microstructure of vertical extrusion direction plane (ND and TD plane) were observed by JEOL JEM-2100 transmission electron microscopy (TEM) and Φ14 mm tem specimens were dealt with to 30–50 μm thickness after mechanical thinning, by ion thinning in Ar gas as shielding gas.

## 3 Results and discussion

### 3.1 Grain morphology

Figure 3 shows the grain morphology of the products obtained by AFE at different forming temperatures. Figures 3(a)–3(c) show the grain structure perpendicular to the ED (ND and TD plane). According to the linear intercept method measured, the average grain sizes of 573, 623 and 673 K were 3.91, 6.49 and 10.96 μm, respectively.

Figure 3 shows that the DRX occurred during AFE at different temperatures. However, the grain size has grown to some extent with the increase of temperature. Figures 3(d)–3(f) illustrate a unique grain color map of AZ31 magnesium alloy processed with AFE along the extrusion direction plane (ED and TD plane) at different temperatures. Different colors represent different grains rather than different orientations. To improve the accuracy of the results, the grains less than 4 μm are cleared and the grain tolerance angle is 5°.

The microstructure is homogeneous and consists of small equiaxial grains when the forming temperature is 573 K. A small amount of banded structure along the extrusion direction can be seen clearly. Along the banded structure grain boundary distributes relatively small equiaxial grains. The results show that grain refinement caused by strain and grain growth caused by high temperature of AFE have basically reached dynamic balance. There is a coarse banded structure and the recrystallized grains along the

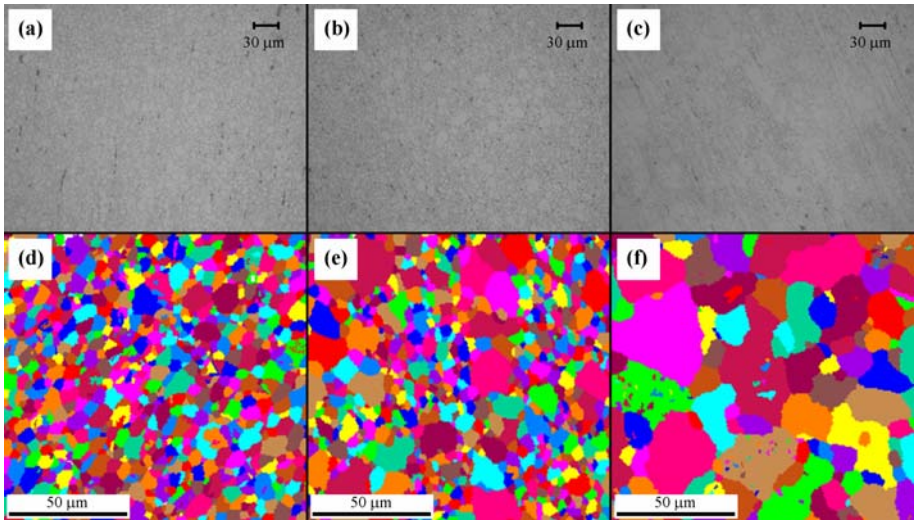


**Fig. 3** Microstructure of the different extrusion direction at different temperatures: **(a)** perpendicular to the ED (ND and TD plane) at 573 K; **(b)** perpendicular to the ED (ND and TD plane) at 623 K; **(c)** perpendicular to the ED (ND and TD plane) at 673 K; **(d)** along the extrusion direction plane (ED and TD plane) at 573 K; **(e)** along the extrusion direction plane (ED and TD plane) at 623 K; **(f)** along the extrusion direction plane (ED and TD plane) at 673 K.

edge obviously grew when the forming temperature is up to 673 K.

### 3.2 Grain orientation

Figure 4 shows the grain orientation maps and misorientation angles with different temperatures. Figures 4(a)–4(c) reveal the grain orientation images of 573, 623 and 673 K, respectively. Each color on the maps indicates a crystallographic orientation. The red color represents the grains which parallel to the basal surface. The grains gradually rotate relative to the (0001) planes during the AFE process at different temperatures; therefore, it is not easy to form the CE texture which has great significance to reduce the anisotropy of extrusion extrudate.

Figures 4(d)–4(f) show the misorientation angle distribution images of 573, 623 and 673 K, respectively. To ensure credible results, the misorientation angles less than 2° are not calculated. Some studies have found that recrystallization grains often have high grain boundaries [21]. The fraction of high-angle grain boundaries (HAGBs) gradually decreases with the increase of temperature. Due

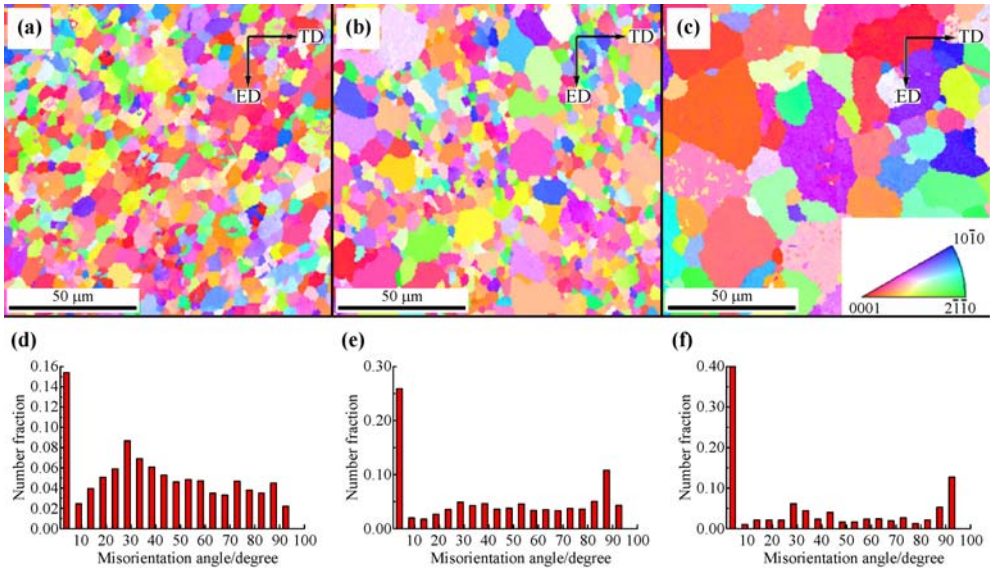


**Fig. 4** The orientation maps of **(a)** 573 K, **(b)** 623 K and **(c)** 673 K. The misorientation angles of **(d)** 573 K, **(e)** 623 K and **(f)** 673 K.

to the increase of the temperature, the small grains of DRX in the AFE process will absorb the energy and grow to a certain extent. Compared with the forming conditions at temperatures of 623 and 673 K, the small grains of DRX at 573 K are retained because the water quenching prevents small grains absorbing energy in time. Therefore, the fraction of HAGBs at 573 K is the most prominent.

### 3.3 Pole figures and inverse pole figures

Figures 5(a)–5(c) show the pole figures (PFs) and inverse pole figures (IPFs) of 573, 623 and 673 K, respectively. The PF show the basal plane texture and most of the grains' basal surface is not parallel to the ED, which is beneficial to activate the basal slip system. With the decrease of the forming temperature, the texture strength decreases and the texture is weakened. This may be because the proportion of DRX is larger than the other two conditions at 573 K, which improves the grain microstructure and weakens the texture intensity. There is no doubt that it is beneficial to improve the performance of the material.

The IPFs are perpendicular to the ND direction (an observation plane composed by TD and ED). The different texture types appear which may be caused by the local strain during the AFE process. The pyramidal planes of $\{10\bar{1}3\}$ and $\{10\bar{1}1\}$ are parallel to the observation plane. The intensities are: $\{10\bar{1}3\} > \{10\bar{1}1\}$. The texture weakening is beneficial to reduce the anisotropy during the AFE process of AZ31 magnesium alloy, which can improve the ability of plastic forming.

### 3.4 Mechanical properties and fracture morphology

Figures 6(a) and 6(b) show the tensile sample pictures before and after the tensile samples fracture. Figure 6(c) presents the comparison of mechanical properties, including the tensile strength (TS), the yield strength (YS) and the elongation.

In the temperature range of 573–673 K, the YS, TS and elongation of the extruded extrudate decreased with increasing the forming temperature. At temperatures of 573, 623 and 673 K, the YS values of extruded extrudate

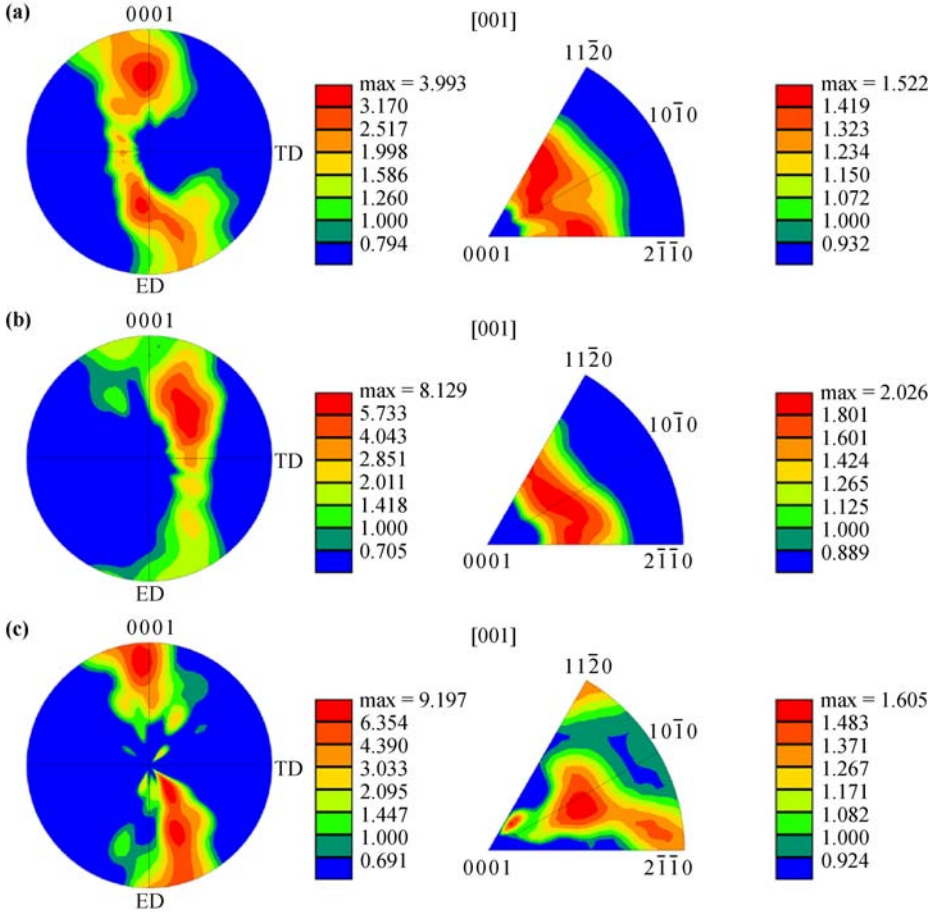


**Fig. 5** Texture evolution under different temperatures: **(a)** 573 K; **(b)** 623 K; **(c)** 673 K.

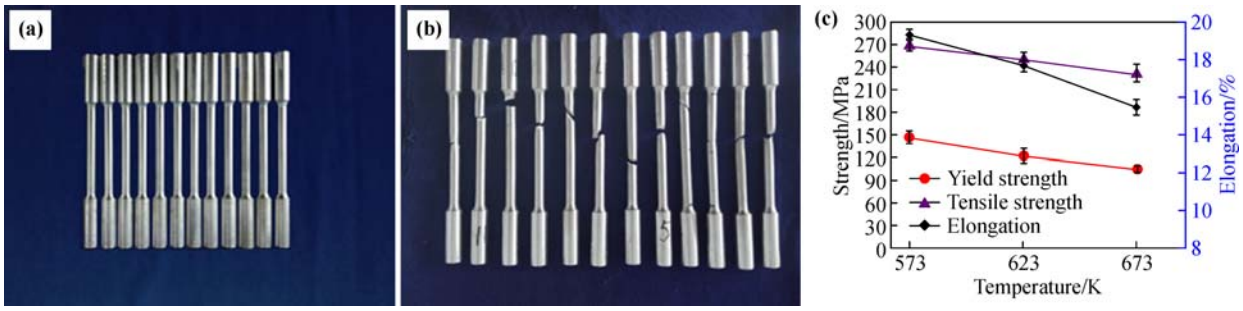


**Fig. 6** The tensile samples **(a)** before and **(b)** after fracture. **(c)** The comparison of mechanical properties.

are 145.99, 121.63 and 105.38 MPa, respectively, while the TS values are 268.48, 250.58 and 230.61 MPa, respectively. By contrast, YS and TS of the corresponding reduced 27.82% and 14.11%, and the elongation reduced from 19.3% to 15.5% when the temperature was from 573 to 673 K.

Figure 7 shows the fracture morphology of the extruded extrudate at different temperatures observed by SEM, which is beneficial to understand the change of mechanical properties.

Figures 7(a) and 7(d) show fracture morphologies which magnified 20 and 200 times at 573 K, respectively. The fracture surface has a large number of dimples and almost no brittle fracture surface and cleavage step exist, which is mainly manifested as ductile fracture. Figures 7(b) and 7(e) show fracture morphology which magnified 20 and 200 times at 623 K, respectively. Compared with the former, dimple number and depth significantly decrease and appear some cleavage steps; therefore, the elongation is lower than that at 573 K. Figures 7(c) and 7(f) show fracture morphology which magnified 20 and 200 times at 673 K, respectively. The fracture surface has a large amount of cleavage step and tear ridge. The fracture surface of the specimen is irregular and almost no dimples exist, which is mainly manifested as brittle fracture. The elongation is lower than those at other temperatures because the grain size is very coarse and the distribution is very inhomogeneous at 673 K.

### 3.5 Mechanism analysis

Figure 8 shows TEM images at different temperatures.

Figure 8(a) show the grain morphology of the as-cast AZ31 magnesium alloy at 573 K. Small equiaxed grains exist in sample which is due to DRX. By the grain morphology can be seen that different directions dislocation tangle seriously in grains. According to the analysis, the small grain shown in Fig. 8(b) should be separated from the elongated grains which provide strong evidence for DRX in the AFE process. It is precisely because of the role of DRX, the grain microstructure of 573 K becomes smaller and more homogeneous.

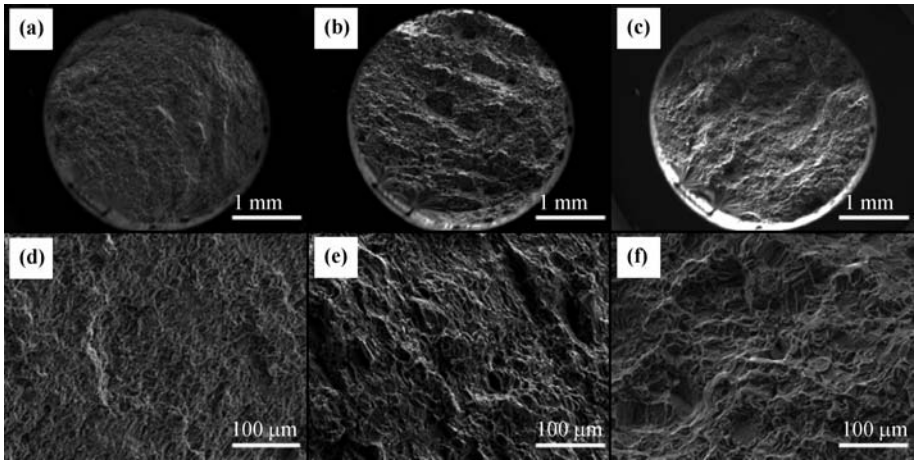


**Fig. 7** The fracture morphologies: **(a)** magnified 20 times at 573 K; **(b)** magnified 20 times at 623 K; **(c)** magnified 20 times at 673 K; **(d)** magnified 200 times at 573 K; **(e)** magnified 200 times at 623 K; **(f)** magnified 200 times at 673 K.

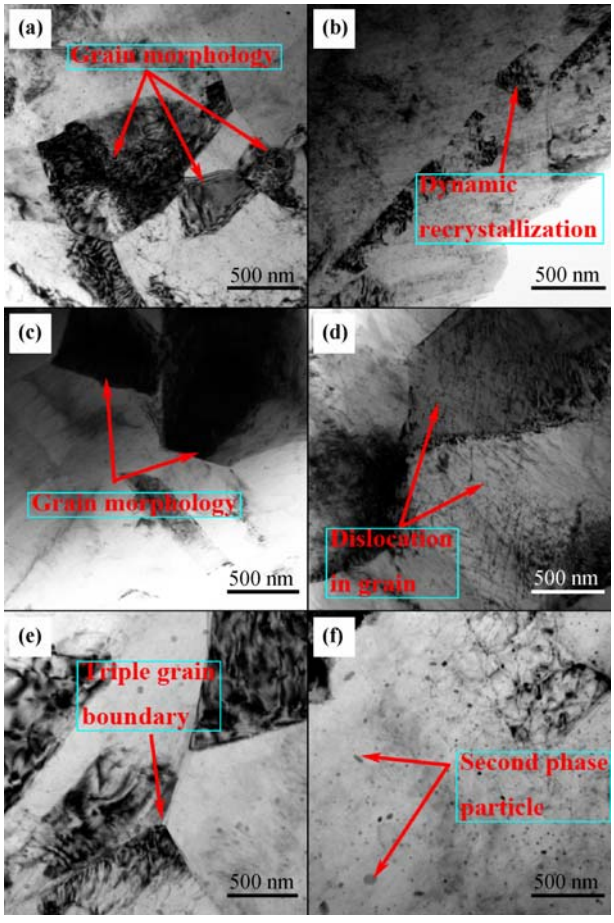


**Fig. 8** TEM images: **(a)** grain morphology at 573 K; **(b)** dynamic recrystallization at 573 K; **(c)** grain morphology at 623 K; **(d)** dislocation in grain at 623 K; **(e)** triple grain boundary at 673 K; **(f)** second phase particle at 673 K.

Figure 8(c) show the grain morphology at 623 K. It can be seen that the size of small grains is obviously larger than that at 573 K. The reason is that the small grains of DRX gradually grow up due to the increase of the forming temperature. The dislocation density revealed in Fig. 8(d) is smaller than that at 573 K, thus the TS of the extruded product decreases. The grain boundary has a tendency to transform into HAGBs through absorbing dislocation.

Figure 8(e) show the grain morphology at 673 K. Due to the influence of the temperature, the refined grains absorb so enough energy that become coarse and the grain boundaries are flat. Under this condition, the effect of temperature has exceeded the grain refinement. As shown in Fig. 8(f), the second phase particles are dispersed in the samples. The precipitated particles in the nanometer scale are of different shapes, such as ellipsoidal, prismatic, lath shape and so on. Due to the influence of temperature rise, the mechanical properties of extruded products are less than those at 573 K.

### 3.6 DRX characterization

There are several details in the magnified orientation maps that provide solid evidence to support the occurrence of DRX during AFE processing at 573 K are shown in Fig. 9.

As can be seen in Fig. 9(a), the unit cells rotate slightly in a certain manner from the new formed fine grains of DRX to the coarse grains due to gradually absorbing energy. This gradual lattice rotation induced during AFE is believed to be DRX. Moreover, in relatively coarse grains frequently find the low-angle grain boundaries (LAGBs) marked by arrows A for white lines in Fig. 9, which agree with the continuous formation of LAGBs by absorbing dislocations (Fig. 8(b)). More careful investigation shows that new HAGBs are formed by the progressive evolution of LAGBs, which can be revealed from the fact that incomplete HAGBs are connected by LAGBs (examples are marked by arrow B in Figs. 9(b)–9(d)).

## 4 Conclusions

1) It is equivalent to the part of the punches contact with billet during AFE processing. The forming load was significantly reduced because the actual loading function area decreased compared with CE. The unique loading method of two punches alternately loading change the metal flow behavior and order in the mold cavity. In the AFE process we design the oriented die to avoid the occurrence of the bending defects.

2) The research results show that the AZ31 magnesium alloy grains are fine and homogeneous at 573 K during AFE processing. There is a coarse banded structure and the recrystallized grains along the edge obviously grew when the forming temperature is up to 673 K. The fraction of HAGBs gradually decreases with increasing the temperature according to the comparison of the grain boundary angle distribution.

3) The YS, TS and elongation of the extruded extrudate decreased with increasing the forming temperature. By contrast, YS and TS of the corresponding reduced 27.82% and 14.11%, and the elongation reduced from 19.3% to 15.5% when the temperature was from 573 to 673 K. The fracture mode is transformed from ductile fracture to brittle fracture according to the fracture morphology.

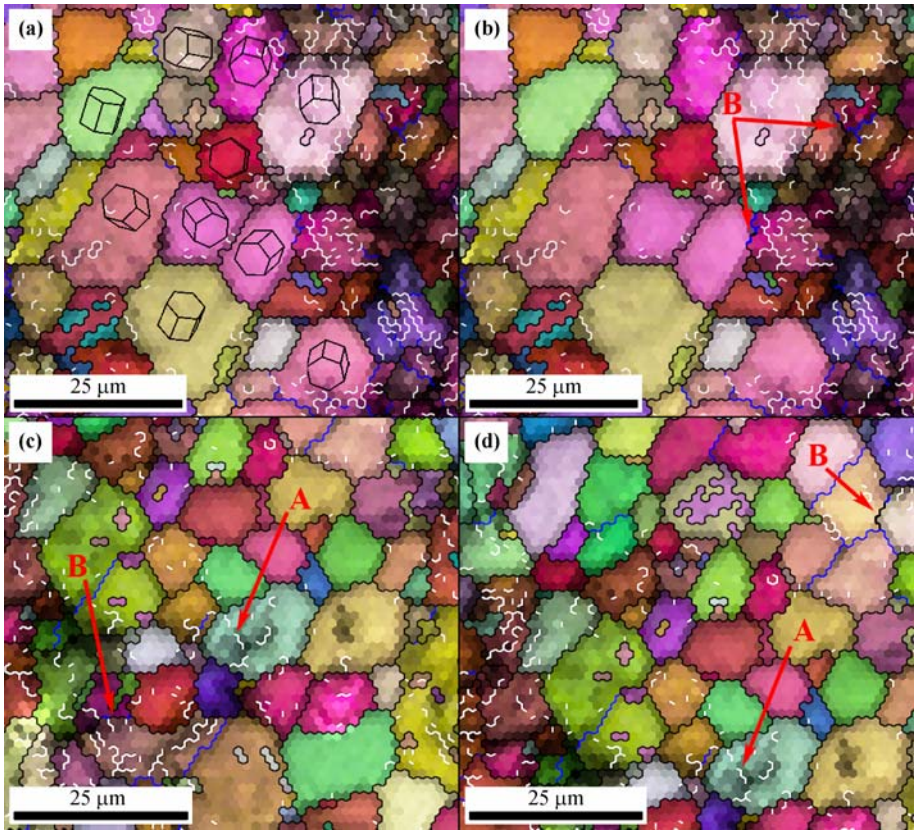


**Fig. 9** The solid evidence of DRX: **(a)** orientation map with superimposed hcp unit cells magnified from Fig. 4(a); **(b)(c)(d)** orientation maps magnified from Fig. 4(a), LAGBs in grains and the examples which indicate that HAGBs are connected by LAGBs (HAGBs are marked with black lines while LAGBs with misorientations of (2°–5°) and (5°–15°) are marked with white and blue lines, respectively).

4) The microstructure is homogeneous and consists of small equiaxial grains due to the effect of DRX at 573 K. The small grains of DRX gradually grow up and dislocation density significantly decreased due to increasing the forming temperature, leading to the TS of the extruded extrudate decrease. The second phase particles with different shapes are dispersed in the samples to further reduce the comprehensive performance.

**Acknowledgement** This project was supported by the National Natural Science Foundation of China (Grant No. 51675143).

## References

[1] Joost W J, Krajewski P E. Towards magnesium alloys for high-volume automotive applications. Scripta Materialia, 2017, 128: 107–112

[2] Chen Q, Zhao Z, Chen G, et al. Effect of accumulative plastic deformation on generation of spheroidal structure, thixoformability and mechanical properties of large-size AM60 magnesium alloy. Journal of Alloys and Compounds, 2015, 632: 190–200

[3] Zhao Z D, Chen Q, Chao H Y, et al. Microstructural evolution and tensile mechanical properties of thixoforged ZK60-Y magnesium alloys produced by two different routes. Materials & Design, 2010, 31(4): 1906–1916

[4] Alizadeh R, Mahmudi R, Ngan A H W, et al. Microstructure, texture, and superplasticity of a fine-grained Mg–Gd–Zr alloy processed by equal-channel angular pressing. Materials Science and Engineering A, 2016, 47(12): 6056–6069

[5] Lin J B, Wang X Y, Ren W J, et al. Enhanced strength and ductility due to microstructure refinement and texture weakening of the GW102K alloy by cyclic extrusion compression. Journal of Materials Science and Technology, 2016, 32(8): 783–789

[6] Figueiredo R B, Langdon T G. Development of structural heterogeneities in a magnesium alloy processed by high-pressure torsion. Materials Science and Engineering A, 2011, 528(13–14): 4500–4506

[7] Fata A, Faraji G, Mashhadi M M, et al. Hottensile deformation and fracture behavior of ultrafine-grained AZ31 magnesium alloy processed by severe plastic deformation. Materials Science and Engineering A, 2016, 674: 9–17

[8] Wang Q, Chen Y, Liu M, et al. Microstructure evolution of AZ series magnesium alloys during cyclic extrusion compression. Materials Science and Engineering A, 2010, 527(9): 2265–2273

[9] Kaseem M, Chung B K, Yang H W, et al. Effect of deformation temperature on microstructure and mechanical properties of AZ31 Mg alloy processed by differential-speed rolling. Journal of Materials Science and Technology, 2015, 31(5): 498–503

[10] Li F, Zeng X, Cao G J. Investigation of microstructure characteristics of the CVCDEed AZ31 magnesium alloy. Materials Science and Engineering A, 2015, 639: 395–401

[11] Sepahi-Boroujeni S, Fereshteh-Saniee F. Expansion equal channel angular extrusion, as a novel severe plastic deformation technique. Journal of Materials Science, 2015, 50(11): 3908–3919

[12] Hu H J, Wang H, Zhai Z Y, et al. The influences of shear deformation on the evolutions of the extrusion shear for magnesium alloy. International Journal of Advanced Manufacturing Technology, 2014, 74(1–4): 423–432

[13] Orlov D, Raab G, Lamark T T, et al. Improvement of mechanical properties of magnesium alloy ZK60 by integrated extrusion and equal channel angular pressing. Acta Materialia, 2011, 59(1): 375–385

[14] Orlov D, Ralston K D, Birbilis N, et al. Enhanced corrosion resistance of Mg alloy ZK60 after processing by integrated extrusion and equal channel angular pressing. Acta Materialia, 2011, 59(15): 6176–6186

[15] Shahbaz M, Pardis N, Ebrahimi R, et al. A novel single pass severe plastic deformation technique: Vortex extrusion. Materials Science and Engineering A, 2011, 530(1): 469–472

[16] Yang X, Miura H, Sakai T, et al. Dynamic evolution of new grains in magnesium alloy AZ31 during hot deformation. Materials Transactions, 2003, 44(1): 197–203

[17] Yang Q, Jiang B, Tian Y, et al. A tilted weak texture processed by an asymmetric extrusion for magnesium alloy sheets. Materials Letters, 2013, 100: 29–31

[18] Yang Q, Jiang B, He J, et al. Tailoring texture and refining grain of magnesium alloy by differential speed extrusion process. Materials Science and Engineering A, 2014, 612: 187–191

[19] Wang C P, Li F G, Li Q H, et al. Numerical and experimental studies of pure copper processed by a new severe plastic deformation method. Materials Science and Engineering A, 2012, 548(3): 19–26

[20] Khoddam S, Farhoumand A, Hodgson P D. Axi-symmetric forward spiral extrusion, a kinematic and experimental study. Materials Science and Engineering A, 2011, 528(3): 1023–1029

[21] Al-Samman T, Li X, Chowdhury S G. Orientation dependent slip and twinning during compression and tension of strongly textured magnesium AZ31 alloy. Materials Science and Engineering A, 2010, 527(15): 3450–3463